

## Geology

### Quantitative analysis of seismogenic shear-induced turbulence in lake sediments

Nadav Wetzler, Shmuel Marco and Eyal Heifetz

*Geology* 2010;38;303-306

doi: 10.1130/G30685.1

---

#### Email alerting services

click [www.gsapubs.org/cgi/alerts](http://www.gsapubs.org/cgi/alerts) to receive free e-mail alerts when new articles cite this article

#### Subscribe

click [www.gsapubs.org/subscriptions/](http://www.gsapubs.org/subscriptions/) to subscribe to *Geology*

#### Permission request

click <http://www.geosociety.org/pubs/copyrt.htm#gsa> to contact GSA

Copyright not claimed on content prepared wholly by U.S. government employees within scope of their employment. Individual scientists are hereby granted permission, without fees or further requests to GSA, to use a single figure, a single table, and/or a brief paragraph of text in subsequent works and to make unlimited copies of items in GSA's journals for noncommercial use in classrooms to further education and science. This file may not be posted to any Web site, but authors may post the abstracts only of their articles on their own or their organization's Web site providing the posting includes a reference to the article's full citation. GSA provides this and other forums for the presentation of diverse opinions and positions by scientists worldwide, regardless of their race, citizenship, gender, religion, or political viewpoint. Opinions presented in this publication do not reflect official positions of the Society.

---

#### Notes

# Quantitative analysis of seismogenic shear-induced turbulence in lake sediments

Nadav Wetzler, Shmuel Marco, and Eyal Heifetz

Department of Geophysics and Planetary Sciences, Tel Aviv University, Tel Aviv, Israel

## ABSTRACT

Spectacular deformations observed in lake sediments in an earthquake prone region (Lisan Formation, pre-Dead Sea lake) appear in phases of laminar, moderate folds, billow-like asymmetric folds, coherent vortices, and turbulent chaotic structures. Power spectral analysis of the deformation indicates that the geometry robustly obeys a power-law of  $-1.89$ , similar to the measured value of Kelvin-Helmholtz (KH) turbulence in other environments. Numerical simulations are performed using properties of the layer materials based on measurements of the modern Dead Sea sediments, which are a reasonable analogue of Lake Lisan. The simulations show that for a given induced shear, the smaller the thickness of the layers, the greater is the turbulent deformation. This is due to the fact that although the effective viscosity increases (the Reynolds number decreases) the bulk Richardson number becomes smaller with decrease in the layer thickness. The latter represents the ratio between the gravitational potential energy of the stably stratified sediments and the shear energy generated by the earthquake. Therefore, for thin layers, the shear energy density is larger and the KH instability mechanism becomes more efficient. The peak ground acceleration (PGA) is related to the seismogenic shear established during the earthquake. Hence, a link is made between the observed thickness and geometry of a deformed layer with its causative earthquake's PGA.

## INTRODUCTION

Earthquake-induced deformation of sediments, called seismites, is common in the late Pleistocene lacustrine Lisan Formation near the Dead Sea (Fig. 1). El-Isa and Mustafa (1986) postulated that the abundant folds formed when seismic waves deformed the sediments at the lake bed. The discovery of turbulent breccia layers (originally called "mixed layers") abutting syndepositional faults (Agnon et al., 2006; Marco and Agnon, 1995) proved that the breccia layers are seismites, thus providing a paleoseismic record spanning 70–15 ka (Marco et al., 1996). Additional confirmation for the identification of these layers as seismites was found in the temporal correlation of late Holocene breccias with historical earthquakes (Ken-Tor et al., 2001; Migowski et al., 2004). The deformation features typically appear in layers with thickness varying from centimeters to decimeters. The layers are folded asymmetrically in trains showing the same trend of axial plane dips. The deformed beds are enclosed between undeformed layers of alternating millimeter-scale laminas with annual pairs of winter detritus and summer evaporitic aragonite (Begin et al., 1974).

The tectonic environment of an active plate boundary in which these layers lay, suggests that understanding the process of seomite formation might provide a method to relate sediment deformation features with earthquake parameters. The original sediments consist of stably stratified water saturated mud. This condition rules out the role of Rayleigh-Taylor Instability (requiring an inversion of densities). The asso-

ciation of a specific mechanical process with the seismites under discussion was first presented by Heifetz et al. (2005), who hypothesized that, since earthquakes typically induce shear and the sediments are stably stratified, Kelvin Helmholtz Instability (KHI) is a plausible mechanism. Using linear stability analysis they showed that strong earthquakes are indeed capable of setting off the KHI, by providing shear kinetic energy that exceeds the gravitational potential energy. While the analysis of Heifetz et al. (2005) was linear, it is evident that nonlinear processes play a major role in the dynamics of strong earthquakes, which is the focus of this paper. We further examine the response of stably stratified mud to an imposed shear through direct numerical simulation (DNS), and uses the KHI hypothesis to explore the possibility of using these structures as "paleoseismograms."

## POWER SPECTRUM ANALYSIS

The sediment deformations in the study area (left column of Fig. 2) appear in various forms of linear waves, billow-like asymmetric folds, coherent vortices, and turbulent chaotic structures (breccia).

Because KHI is a non-isotropic phenomena (with vertical stratification and shear and horizontally directed velocities) its energy power spectrum does not obey the inertial isotropic Kolmogorov turbulence power law  $[E(k) \sim k^{-a}]$ , where  $E(k)$  is the energy deposited in wave number  $k = 2\pi/\lambda$ , where  $\lambda$  is the wavelength, with  $a = 5/3$ . In other disciplines, such as ocean fluid dynamics (e.g., Li and Yamazaki, 2001), turbulent KHI was found to obey a power law

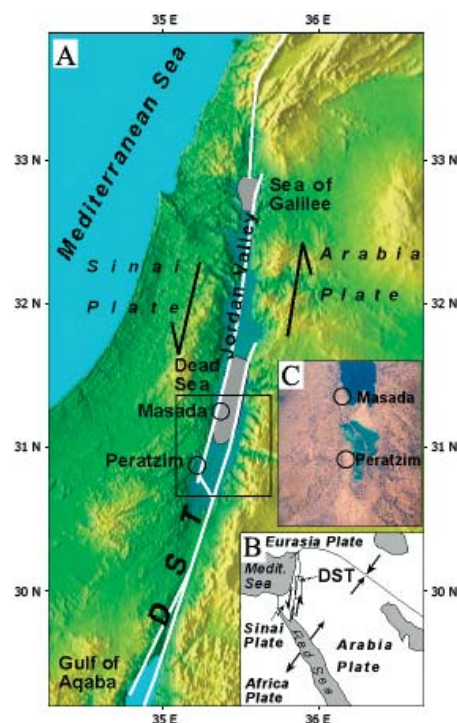


**Figure 1.** A: Sampling locations shown with the background of maximum extent of Lisan at 26 ka in blue. B: Tectonic plates in the Middle East. Dead Sea Transform (DST) transfers the opening motion in the Red Sea to the Taurus-Zagros collision zone. C: Landsat image of sampling region.

with a value of  $\sim 2$ . Hence, in order to examine further the KHI hypothesis, we first analyze the power spectra of hundreds of observed deformations in the field.

Unlike analyses of KHI in lab or field experiments, in which the power spectrum of the kinetic and potential energy are measured directly, we have to deduce the energy indirectly from the motionless deformed layers. After the deformation ceased, the water was squeezed out of the sediment, which became solid rock. Hence, as a proportional proxy for the potential energy during the dynamic stage (i.e., the earthquake) we consider the deformation amplitude squared ( $A^2$ ), defined in Figure 3. Since in idealized KHI the energy is equally partitioned between its kinetic and potential components (e.g., Kundu and Cohen, 2008) it can be approximately related to the eddy kinetic energy.

We photographed more than 300 folds of all shapes and evolutionary stages in the Lisan

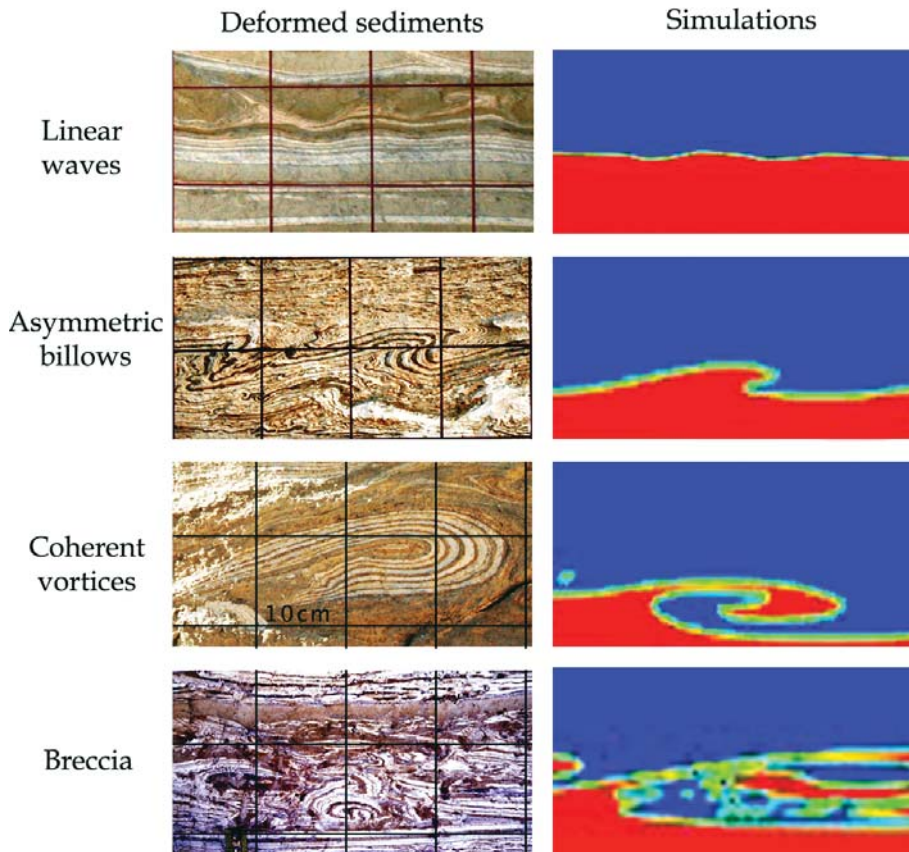


Figure 2. Comparison of field observations in Lisan Formation sediments with numerical simulations showing similar stages of Kelvin-Helmholtz instability evolution from linear wave through asymmetric billows, coherent vortices, and fully turbulent breccia. Grid spacing on photos is 10 cm.

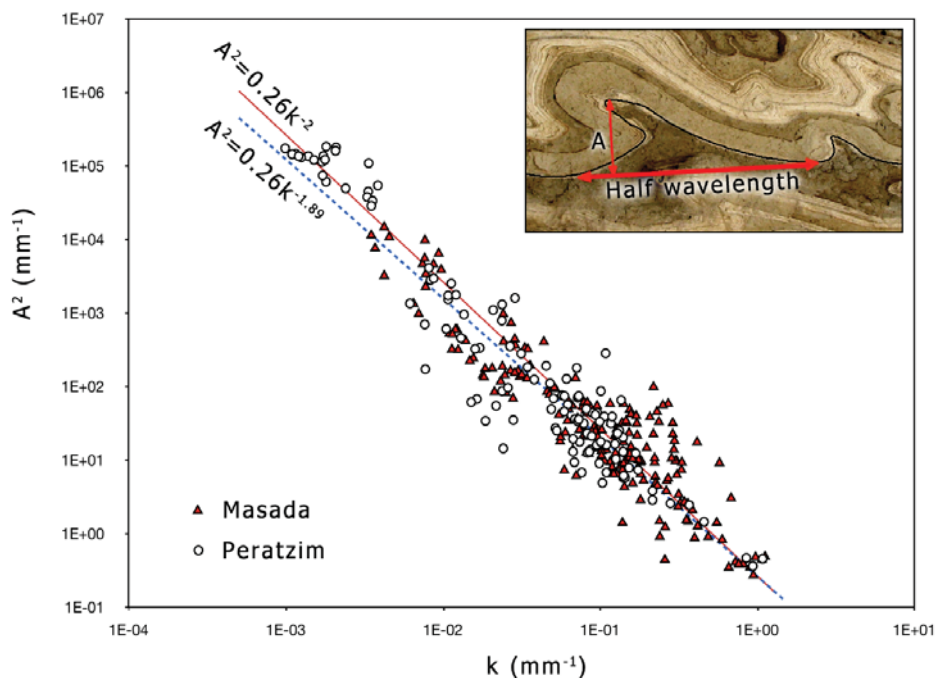


Figure 3. The deformation amplitude ( $A$ ) squared versus wavenumber  $k$  of 310 folds measured in Masada (solid triangles) and Peratzim (open circles). The dashed blue regression line of  $A^2 = 0.26k^{1.89}$ ,  $R^2 = 0.98$ , is compared with a reference curve of  $A^2 = 0.26k^2$  (solid). Inset picture at top right illustrates how the amplitudes and wavelengths were measured.

Formation outcrops in two locations, Masada and Peratzim (Fig. 1). For each fold the most conspicuous lamina is traced and stored in a digital database. For scaling and rectification, we use a  $1\text{ m} \times 1\text{ m}$  frame with grid lines spaced by 10 cm as well as a ruler with millimeter marks. For very small folds we counted pixels on images using standard commercial image processing software. Each measurement includes the deformation amplitude  $A$ , from the base of the lamina to the most upper part of its curved wave structure. The half wavelength ( $\lambda/2$ ) is measured on the base of the lamina between the two minima points (illustrated on inset in Fig. 3). Although this measurement technique is rather crude the power spectrum is strikingly robust with a power law of 1.89 and  $R^2 = 0.98$ .

The robustness of the power law and its agreement with the measured KHI power law in other disciplines, together with the facts that these hundreds of samples (with amplitudes and associated wavelengths varying from scales of centimeters to decimeters) are associated with dozens of different earthquake events, and are taken from two different sites, all suggest that KHI is likely the governing mechanism of the sediment deformation.

#### DIRECT NUMERICAL SIMULATIONS OF KHI

Since the observed power spectra, and the linear stability analysis both support the KHI hypothesis, we proceed with direct numerical simulations (DNS) examining the response of stably stratified saturated mud to an imposed shear. This response depends on the material properties of the mud, mostly on its density and viscosity profiles. In order to obtain a reasonable estimation of the paleo-Lake Lisan mud properties we use the modern Dead Sea sediments as an analogue.

The purpose of these simulations is to verify whether the deformations observed in the field can be generated by KHI, given typical earthquake properties (duration on the order of seconds, ground acceleration  $\sim 0.1\text{ g}$ , where  $g$  is gravity), typical layer thickness (from a few centimeters up to 0.5 m), and typical density and viscosity stratifications. As a best reasonable estimation for the latter two properties, we sampled mud from the Dead Sea lake bed at two layers: at depths of 10 cm and 30 cm. The average densities are  $1600\text{ kg/m}^3$  for the upper layer and  $1750\text{ kg/m}^3$  for the lower layer, where their respective viscosities (measured with a Newtonian analog viscometer) are 0.3 PaS and 3 PaS.

We use the FLUENT commercial software (<http://www.ansys.com/products/fluid-dynamics/fluent/>) to solve the Navier-Stokes equations numerically. The simulation setup is composed of two stratified fluid layers, subject to shear. In the simulations the layers are 2 m long and their

thickness varies between 4, 10, and 50 cm. The model grid is built using the GAMBIT software, with a fixed horizontal resolution of 0.5 cm and a vertical resolution of 0.1, 0.3, and 1 cm respectively. The background hydrostatic pressure is taken to be 600,000 Pa corresponding to a 50 m lake depth, based on paleo lake level record (Bartov et al., 2002). To study the two-phase problem with the FLUENT simulations we applied the option of fluid volume conservation, free boundary condition at the interface between the layers, and no slip solid boundary conditions for the upper and lower boundaries.

The upper layer is accelerated horizontally, with respect to the lower layer, imposing a range of accelerations of 0.1, 0.2, 0.3, and 0.6 g. A localized sinusoidal perturbation with a frequency of 1 Hz (representing a seismic wave) is initiated at the interface with small amplitude of 5 mm. The time step of the simulation is 0.01 s and the simulations are run up to 1.5 s.

Snapshots after 1 s of evolution of these 12 runs are presented in Figure 4A. The four types of deformation found in the field (linear waves, asymmetric billows, coherent vortices, and fully turbulent breccia layers) are produced by the simulations. The resemblance of the simulations to the observed deformations is apparent in Figure 2. The larger the ground acceleration and the thinner the layer, the more intense is the deformation. While the former dependency is quite obvious, the latter is not trivial, although predicted by Heifetz et al. (2005) by the linear analysis. On the one hand, the viscosity becomes more effective for thin layers since the Reynolds number ( $Re = UD/v$ , where  $U$  is the characteris-

tic velocity,  $D$  is the layer thickness and  $v$  is the kinematic viscosity) becomes smaller. On the other hand, the bulk Richardson number ( $Ri$ ) becomes smaller as well [ $Ri = (g\Delta\rho/\rho_m\Delta U^2)D$ , where  $\Delta\rho$  is the density difference between the layers and  $\rho_m$  is their mean value]. The Richardson number indicates the ratio between the gravitational potential energy of the stably stratified sediments and the required shear energy, exerted by the earthquake, to overcome the former. Because the sheared region is concentrated at the interface between the layers but acts to deform the full depth of the layers, the shear energy density is larger for thin layers, making the KHI mechanism more efficient.

The deformation stages as a function of Richardson and Reynolds numbers are summarized in Figure 4. As expected from the theory, no instability is obtained when  $Ri > 0.25$ .

## DISCUSSION

The ubiquitous appearance of deformed coherent billows, together with the basic conditions of stably stratified sediments subjected to earthquake-induced shear, strongly suggest that KHI is indeed the governing mechanism of fold evolution. Nonetheless, it is impossible to absolutely determine that the seismite deformations examined in this study resulted only from KHI during paleo-earthquakes.

Among other plausible mechanisms is the liquefaction of the underlying muddy layer and passive collapse of the overlying cohesive mud during the earthquake (Owen, 1987). Then, even slopes with slight inclination can yield asymmetrical morphologies. Evidence for simi-

lar KHI-induced deformations in other places were observed after the tsunami generated by the great Sumatra earthquake (Matsumoto et al., 2008), where coherent billows were formed at the sheared interface at the bottom of the tsunami sand deposits. Simulations of the effects of strong earthquakes in Lake Lisan also show that seiches may form and cause destratification in the water column associated with breccia forming at the lake bottom (Begin et al., 2005). Hence, the seiche-induced shear at the bottom of the lake could have enhanced the turbulent characteristics of the deformation. Another case was observed in deformed clay sediments that also show coherent billows in the Jharia Basin, India. It was shown experimentally and numerically by Dasgupta (2008), that the waveform of shear induced deformation is enhanced if the two layers have different rheological properties.

A detailed analysis of the deformation amplitude power spectrum of more than 300 samples (in varying sizes of few millimeters to 1 m), taken from two different sites near the Dead Sea, triggered by dozens of different earthquakes, reveals a strikingly well-constrained sharp power law of 1.89, a similar value to the power law obtained for KHI in other environments.

Although it is impossible to determine the Ozmidov scale, from which the stratification shifts the power spectrum from the inertial Kolmogorov power law to the KH one, this finding strongly supports the KHI hypothesis (the Ozmidov scale is defined as the square root of the ratio between the dissipation rate of turbulent kinetic energy and the third power of the

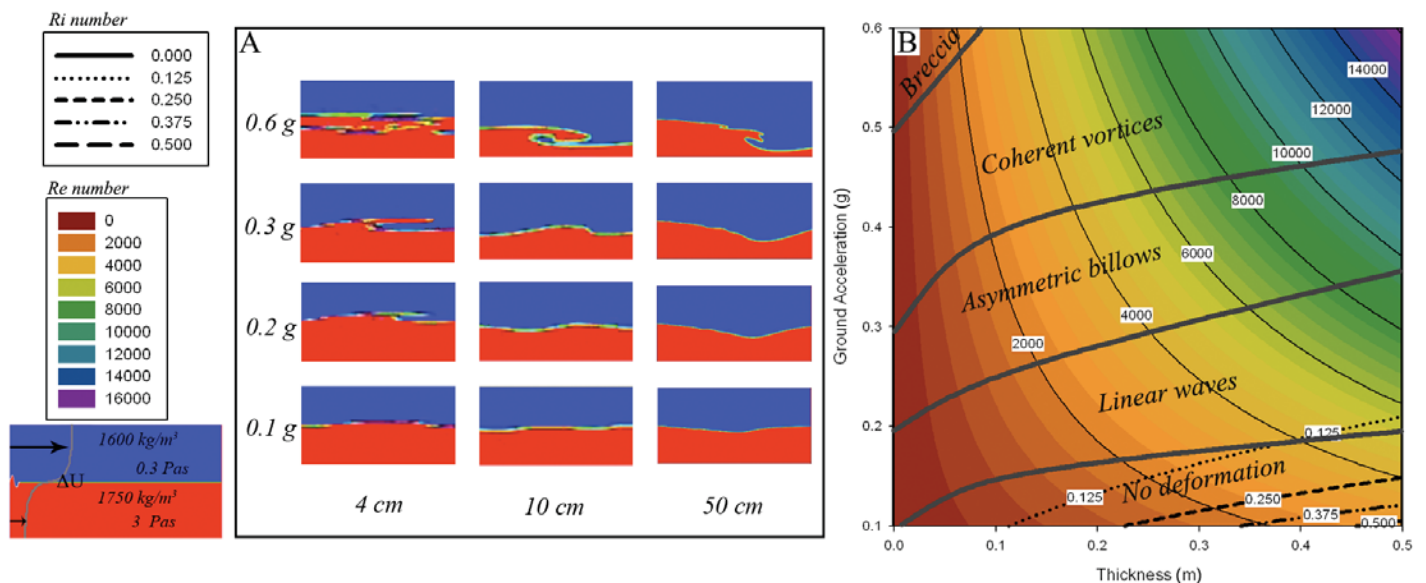


**Figure 4. A:** Simulation snapshots after 1 s from onset of earthquake first shock for different ground accelerations and various layer thickness. Basic simulation setup shown at bottom left. **B:** Values of Reynolds ( $Re$ ; color coded) and Richardson numbers ( $Ri$ ; dashed lines) based on the same layer thickness and ground acceleration as the simulation snapshots on the left (curves are smoothed). Annotation between gray lines indicates ranges with characteristic deformation patterns obtained for each run, after 1 s of model time.

buoyancy frequency. While the buoyancy frequency can be extracted from the density profile there is no reliable way to obtain the dissipation rate from the field data).

Our numerical simulations are somewhat crude. They do not take directly into account the two phase flow non-Newtonian behavior of the consolidated mud, the buildup of pore pressure that may lead to liquefaction, the presence of finite thick shear layer and other related phenomena. Furthermore, the material properties of the sediments (see above) are taken from measurements of the current lakebed sediments, which may differ from the paleo-lake Lisan sediments. Nevertheless, the simulations show that within typical ranges of earthquake ground acceleration, layer thickness, and perturbed seismic frequency, all types of KH deformation phases (linear waves, asymmetric billows, coherent vortices, and fully turbulent breccia layers) are reconstructed. The robustness of the results may therefore testify to the robustness of the KH mechanism.

The numerical simulations indicate that the larger the ground acceleration and the thinner the layer, the more intense are the deformations. The duration of the earthquake was found to affect the geometry, rather than the deformation amplitude. This is somewhat different from the earthquake duration effect on asymmetric morphologies generated by gravity currents above liquefied layers, (Moretti et al., 1999; Owen, 2003).

Potentially, Figure 4 may serve as a sort of "paleoseismogram"; identification of the geometry of the deformation and the layer thickness provides an estimation of the peak ground acceleration. By assuming locations of paleo earthquakes and using known attenuation relations (e.g., Boore et al., 1997) an indirect estimation for the earthquake magnitude may be obtained from the geometrical properties of the deformed sediment layer.

## CONCLUSIONS

We suggest that the various types of deformation in the Lisan Formation can be explained as the results of earthquake triggered KHI. The instability caused a continuous development,

which culminated in turbulent breccias layers. The deformation process was quenched at different stages depending on the sediment properties (layer thickness, density and viscosity gradients) and induced acceleration. These relations may enable the estimation of paleo-earthquake magnitude.

## ACKNOWLEDGMENTS

We thank Amotz Agnon for stimulating discussions and good advice. We are also grateful to Massimo Moretti and an anonymous journal referee for thorough revisions and constructive comments. The research was funded by the Binational U.S.-Israel Science Foundation grant #2004087 to Heifetz and Israel Science Foundation grant 1539/08 to Marco.

## REFERENCES CITED

- Agnon, A., Migowski, C., and Marco, S., 2006, Intraclast breccia layers in laminated sequences: Recorders of paleo-earthquakes, *in* Enzel, Y., et al., eds., *New frontiers in Dead Sea paleoenvironmental research*: Geological Society of America Special Paper 401, p. 195–214.
- Bartov, Y., Stein, M., Enzel, Y., Agnon, A., and Rechtes, Z., 2002, Lake levels and sequence stratigraphy of Lake Lisan, the late Pleistocene precursor of the Dead Sea: *Quaternary Research*, v. 57, p. 9–21, doi: 10.1006/qres.2001.2284.
- Begin, B.Z., Steinberg, D.M., Ichinose, G.A., and Marco, S., 2005, A 40,000 years unchanging of the seismic regime in the Dead Sea rift: *Geology*, v. 33, p. 257–260, doi: 10.1130/G21115.1.
- Begin, Z.B., Ehrlich, A., and Nathan, Y., 1974, Lake Lisan, the Pleistocene precursor of the Dead Sea: *Geological Survey of Israel Bulletin* 63, 30 p.
- Boore, D.M., Joyner, W.B., and Fumal, T.E., 1997, Equations for estimating horizontal response spectra and peak acceleration from western North American earthquakes: A summary of recent work: *Seismological Research Letters*, v. 68, p. 127–153.
- Dasgupta, P., 2008, Experimental decipherment of the soft-sediment deformation observed in the upper part of the Talchir Formation (Lower Permian), Jharia Basin, India: *Sedimentary Geology*, v. 205, p. 100–110, doi: 10.1016/j.sedgeo.2008.01.006.
- El-Isa, Z.H., and Mustafa, H., 1986, Earthquake deformations in the Lisan deposits and seismotectonic implications: *Royal Astronomical Society Geophysical Journal*, v. 86, p. 413–424.
- Heifetz, E., Agnon, A., and Marco, S., 2005, Soft sediment deformation by Kelvin Helmholtz Instability: A case from Dead Sea earthquakes: *Earth and Planetary Science Letters*, v. 236, p. 497–504, doi: 10.1016/j.epsl.2005.04.019.

- Ken-Tor, R., Agnon, A., Enzel, Y., Marco, S., Negendank, J.F.W., and Stein, M., 2001, High-resolution geological record of historic earthquakes in the Dead Sea basin: *Journal of Geophysical Research*, v. 106, p. 2221–2234, doi: 10.1029/2000JB900313.
- Kundu, P.K., and Cohen, I.M., 2008, *Fluid mechanics* (fourth edition): London, Academic Press, 872 p.
- Li, H., and Yamazaki, H., 2001, Observations of a Kelvin-Helmholtz billow in the ocean: *Journal of Oceanography*, v. 57, p. 709–721, doi: 10.1023/A:1021284409498.
- Marco, S., and Agnon, A., 1995, Prehistoric earthquake deformations near Masada, Dead Sea Graben: *Geology*, v. 23, p. 695–698, doi: 10.1130/0091-7613(1995)023<0695:PEDNMD>2.3.CO;2.
- Marco, S., Stein, M., Agnon, A., and Ron, H., 1996, Long term earthquake clustering: A 50,000 year paleoseismic record in the Dead Sea Graben: *Journal of Geophysical Research*, v. 101, p. 6179–6192, doi: 10.1029/95JB01587.
- Matsumoto, D., Naruse, H., Fujino, S., Surphawajraksakul, A., Jarupongsakul, T., Sakakura, N., and Murayama, M., 2008, Truncated flame structures within a deposit of the Indian Ocean tsunami: Evidence of syn-sedimentary deformation: *Sedimentology*, v. 55, p. 1559–1570, doi: 10.1111/j.1365-3091.2008.00957.x.
- Migowski, C., Agnon, A., Bookman, R., Negendank, J.F.W., and Stein, M., 2004, Recurrence pattern of Holocene earthquakes along the Dead Sea transform revealed by varve-counting and radiocarbon dating of lacustrine sediments: *Earth and Planetary Science Letters*, v. 222, p. 301–314, doi: 10.1016/j.epsl.2004.02.015.
- Moretti, M., Alfaro, P., Caselles, O., and Canas, J.A., 1999, Modelling seismites with a digital shaking table: *Tectonophysics*, v. 304, p. 369–383, doi: 10.1016/S0040-1951(98)00289-3.
- Owen, G., 1987, Deformation processes in unconsolidated sands, *in* Jones, M.E., and Preston, R.M.F., eds., *Deformation of sediments and sedimentary rocks*: Geological Society of London Special Publication 29, p. 11–24.
- Owen, G., 2003, Load structures: Gravity driven sediment mobilization in the shallow subsurface, *in* Rensbergen, P.V., et al., eds., *Subsurface sediment mobilization*: Geological Society of London Special Publication 216, p. 21–34.

Manuscript received 14 September 2009

Revised manuscript received 24 October 2009

Manuscript accepted 27 October 2009

Printed in USA